A-K. Schug
(Hamburg University of Technology)

P. Seiler
(University of Minnesota)

H. Pfifer
(University of Nottingham)

E-mail: ann.schug@tuhh.de

DOI: 10.12762/2017.AL13-06

Robustness Margins for Linear Parameter Varying Systems

An approach for extending classical robustness margins to linear parameter varying (LPV) systems is presented. LPV systems are often used to model aircraft dynamics that are highly dependent on the operating conditions such as altitude and airspeed. Classical gain and phase margins are evaluated in the frequency domain and therefore cannot be applied to LPV systems. The proposed approach is based on a time-domain interpretation for disk margins. Specifically, a norm bounded linear time invariant (LTI) uncertainty is interconnected to the nominal LPV system. Next, a time-domain worst-case metric is applied to evaluate both the robustness margin and also the robust performance degradation. The approach does not require detailed uncertainty modeling. In addition, the analysis can be formulated as a convex optimization leading to reliable numerical analysis tools. As an example, the LPV gain margin of a flutter suppression controller for a flexible aircraft is evaluated.

Introduction

This paper presents a method for extending the notion of gain and phase margins to linear parameter varying (LPV) systems. LPV systems are often used in aerospace engineering to model dynamics that strongly depend on the operating conditions, where the state matrices depend on measurable exogenous parameters that vary over time. If the state matrices of the LPV model have a rational dependence on the scheduling parameters, finite dimensional semi-definite programs (SDPs) can be formulated for controller synthesis and analysis [1],[8],[14]. However, in many engineering applications the state matrices have an arbitrary dependence on the parameters. In this case, the analysis and synthesis problem leads to an infinite-dimensional set of linear matrix inequalities (LMIs). A finite approximation approach based on gridding is proposed in [19]. The existing results on LPV modeling, as well as controller design and synthesis have been widely studied and successfully used for many industrial applications. Results on robustness analysis for LPV systems, which depend rationally on the scheduling parameter, can be found, for example, in [18]. However, there is still a gap in the literature when it comes to standard robustness analysis tools for LPV systems with arbitrary parameter dependence. The classical phase and gain margins are evaluated in the frequency domain and can therefore not be applied to LPV systems due to their time varying dynamics. A standard approach is to impose a grid on the scheduling-parameter space and to evaluate the robustness margins at each grid point. However, this does not guarantee the robustness for the entire LPV system. This paper seeks to combine the knowledge about standard robustness margin analysis for linear time invariant (LTI) systems and new results for the analysis of uncertain LPV systems.

Recently, the framework of Integral Quadratic Constraints (IQCs) has gained a lot of attention in the research community. IQCs where first introduced in [7] as a general robustness analysis framework for LTI systems. The authors in [11] propose a time domain interpretation that can be used to extend the IQC framework to LPV systems. Specifically, a worst-case gain metric was proposed to extend the known performance analysis conditions for nominal LPV systems [19] to uncertain LPV systems. Here, the uncertain system is divided into a nominal system and a perturbation block. The IQC can then be imposed on the input/output behavior of the latter. The focus in this paper is on norm bounded LTI uncertainties, used to model simultaneous phase and gain variations in a system. The constraint can be directly obtained by reformulating the norm bound conditions of the uncertainty without having to go into too much detail concerning the IQC framework. The main contributions of this paper are based on the theoretical results in [12]. First, the worst-case metric is used to provide a notion of LPV stability margins. These margins are then used to formulate a simple robustness test for a gain scheduled controller, similar to the classical stability margins in LTI control. Additionally to the single margin point where instability occurs, this new technique can also be used to determine the robust performance of the LPV systems. The theory is finally applied to an aerospace engineering example. Here, the LPV robustness margins of a flutter suppression controller for a flexible aircraft are evaluated and compared to classical LTI analysis results based on μ-theory at each grid point.

Background

In many aerospace applications the dynamics strongly depend on the operating conditions of the aircraft, such as altitude or airspeed. The LPV framework can be used to consider this dependency in the modeling procedure as well as the controller synthesis. The dynamics are expressed as a function of a scheduling parameter. This section provides a brief summary of LPV modeling and introduces the performance of nominal LPV systems. This work is aimed at extending classical (LTI) robustness margins and robust performance analysis to LPV systems. The approach is based on the concept of disk margins for LTI systems as reviewed in Section "Disk Margins for LTI Systems".

Linear Parameter Varying Systems

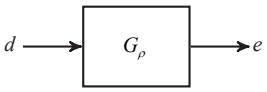

Figure 1 – LPV System

Linear parameter varying (LPV) systems are a special class of time varying systems where the dynamics depend on an exogenous parameter vector $\rho(t)$ restricted to remain in a compact set $\rho(t)\in\mathcal{P}\subset\mathbb{R}^{n_\rho}$ for all $t\geq 0$. An n^{th}-order LPV system G_ρ as depicted in Figure 1 has the form

$$\dot{x}(t)=A\big(\rho(t)\big)x(t)+B\big(\rho(t)\big)d(t) \tag{1}$$
$$e(t)=C\big(\rho(t)\big)x(t)+D\big(\rho(t)\big)d(t)$$

with the continuous functions $A:\mathbb{R}^{n_\rho}\to\mathbb{R}^{n_x\times n_x}$, $B:\mathbb{R}^{n_\rho}\to\mathbb{R}^{n_x\times n_d}$, $C:\mathbb{R}^{n_\rho}\to\mathbb{R}^{n_e\times n_x}$ and $D:\mathbb{R}^{n_\rho}\to\mathbb{R}^{n_e\times n_d}$. In addition, $x(t)\in\mathbb{R}^{n_x}$ is the vector containing the states of the system, $e(t)\in\mathbb{R}^{n_y}$ is the output vector and $d(t)\in\mathbb{R}^{n_u}$ the input vector. Given by the physical restrictions of most practical applications the admissible parameter trajectories are defined by

$$\mathcal{A}:=\left\{\rho:\mathbb{R}^+\to\mathbb{R}^{n_\rho}\,|\,\rho(t)\in\mathcal{P},\ \dot{\rho}(t)\in\dot{\mathcal{P}}\ \forall\, t\geq 0\right\} \tag{2}$$

where the admissible parameter rate is given by the subset

$$\dot{\mathcal{P}}:=\left\{\dot{\rho}\in\mathbb{R}^{n_\rho}\,||\,\dot{\rho}_i\,|\leq\nu_i,\ i=1,\ldots,n_\rho\right\}$$

ν_i is the fastest admissible parameter variation rate.

The performance of an LPV system G_ρ can be measured in terms of the induced $\mathcal{L}_2$-norm. First define the norm of a signal d as $\|d\|_2=\sqrt{\int_0^\infty d^T(t)d(t)dt}$. The set of bounded signals, *i.e.* $d\in\mathcal{L}_2$, are those that satisfy $\|d\|_2<\infty$. The gain of the system from the input d to the output e can be defined using the signal $\mathcal{L}_2$-norm:

$$\|G_\rho\|:=\sup_{0\neq d\in\mathcal{L}_2,\ \rho\in\mathcal{A},\ x(0)=0}\frac{\|e\|_2}{\|d\|_2} \tag{3}$$

A bounded-real type result exists to bound the induced $\mathcal{L}_2$-norm of an LPV system. First, define the following differential operator for a symmetric matrix function $P:\mathcal{P}\to\mathbb{S}^{n_x}$:

$$\partial P(\rho,\dot{\rho})=\sum_{i=1}^{n_\rho}\frac{\partial P(\rho)}{\partial\rho_i}\dot{\rho}_i \tag{4}$$

The theorem below provides a matrix inequality condition to prove stability and bound the induced $\mathcal{L}_2$ gain of an LPV system with bounded parameter variation rate.

Theorem 2.1 (Bounded Real Lemma [20])
An LPV System G_ρ as defined in (1) is exponentially stable and $\|G_\rho\|<\gamma$ if there exists a continuously differentiable symmetric matrix function $P:\mathcal{P}\to\mathbb{S}^{n_x}$ such that the following two conditions hold $\forall(\rho,\dot{\rho})\in\mathcal{P}\times\dot{\mathcal{P}}$

$$P(\rho)>0 \tag{5}$$

$$\begin{bmatrix}P(\rho)A(\rho)+A(\rho)^TP(\rho)+\partial P(\rho,\dot{\rho}) & P(\rho)B(\rho)\\ B(\rho)^TP(\rho) & -I\end{bmatrix}+\frac{1}{\gamma^2}\begin{bmatrix}C(\rho)^T\\ D(\rho)^T\end{bmatrix}\begin{bmatrix}C(\rho) & D(\rho)\end{bmatrix}<0 \tag{6}$$

Proof. This is a standard result but a sketch of the proof is provided since it will be extended for the robustness result. Multiply (6) on the left and right by $\left[x^T,d^T\right]$ and $\left[x^T,d^T\right]^T$, respectively, to obtain (neglecting the dependence on time):

$$\dot{x}^TP(\rho)x+x^TP(\rho)\dot{x}+x^T\partial P(\rho,\dot{\rho})x+\frac{1}{\gamma^2}e^Te-d^Td<0 \tag{7}$$

Define a storage function $V:\mathbb{R}^{n_x}\times\mathcal{P}\to\mathbb{R}^+$ as $V(x,\rho)=x^TP(\rho)x$. Evaluating V along the state and parameter trajectory gives

$$\dot{V}+\frac{1}{\gamma^2}e^Te-d^Td<0 \tag{8}$$

Integrating over the time interval $[0,T]$ and applying $x(0)=0$ yields

$$V(T)+\frac{1}{\gamma^2}\int_0^T e(t)^Te(t)dt-\int_0^T d(t)^Td(t)dt<0 \tag{9}$$

Let $T\to\infty$ and use $V(T)\geq 0$, as well as the definition of the $\mathcal{L}_2$-norm, to obtain bound $\|e\|_2\leq\gamma\|d\|_2$. A slight modification of the arguments (using the compactness of $\mathcal{P}$) yields the strict inequality $\|e\|_2<\gamma\|d\|_2$.

Disk Margins for LTI Systems

In many applications, it is important to provide a high level of robustness. Specifically, the system performance should be insensitive to deviations between the model used for the controller synthesis and the actual system dynamics. Classical robustness measures, e.g., gain and phase margins, can be easily evaluated given the frequency response of the nominal system dynamics. More modern tools, e.g. μ analysis, require more detailed descriptions of the uncertainty. In general, an uncertain system can be described by "pulling out the uncertainty", as shown in Figure 2 [21]. This corresponds to an interconnection of a nominal (not-uncertain) system G and an uncertainty block Δ, as shown in Figure 2. The signals d and e correspond to exogenous inputs and system outputs, respectively. The signals v and w correspond to the signals related to the modeling uncertainty. The notation $F_u(G,\Delta)$ is used to represent this interconnection structure.

As noted above, classical gain and phase margins are common robustness metrics. These margins measure the amount of (individual) gain or phase that can be tolerated before a single closed-loop

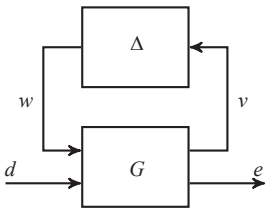

Figure 2 – Uncertain LTI System

becomes unstable. On the other hand, symmetric disk margins, as described in [3, 5], allow for simultaneous variations in both gain and phase within a prescribed disk. The remainder of the section briefly reviews the disk margin concept, since this will be used to formulate the proposed robustness margins for LPV systems. Consider the interconnection shown in Figure 3 where G and K are single input/single output (SISO) LTI systems and Δ is an LTI uncertainty. The symmetric disk margins are related to robustness with respect to this uncertainty interconnection.

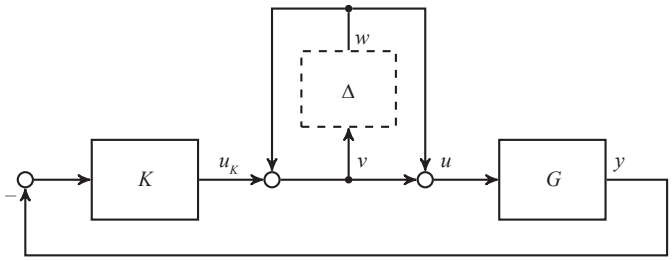

Figure 3 – Input Disk Margin Interconnection

The open loop transfer function, without Δ, from input w to output v is given by $\frac{1}{S_i - T_i}$, where $S_i := \frac{1}{1+GK}$ and $T_i := \frac{GK}{1+GK}$ are the sensitivity and complementary sensitivity functions at the plant input. Thus the disk margin interconnection is equivalent to $F_u\left(\frac{1}{S_i - T_k}, \Delta\right)$ (with no disturbance and error channels). By the small gain theorem [6, 21], the uncertain disk margin interconnection is stable if and only if $\|\Delta\|_\infty < \left\|\frac{1}{S_i - T_i}\right\|_\infty$. Thus, the stability radius (margin) can be defined as $r := 1/\|S_i - T_i\|$ where $0 < r < 1$ typically satisfies $0 < r < 1$.

Block diagram manipulation can be used to bring the disk margin interconnection into the equivalent form shown in Figure 4. This alternative form provides a useful connection back to classical gain and phase margins. This implies that the interconnection is stable for all real gains from u_K to u in the interval $\left[\frac{1-r}{1+r}, \frac{1+r}{1-r}\right]$. This proves the following symmetric lower and upper disk gain margins:

$$\mathrm{GM}_l = \frac{1-r}{1+r}, \quad \mathrm{GM}_u = \frac{1+r}{1-r} \tag{10}$$

Similarly, stability of Figure 4 for all $\|\Delta\|_\infty < r$ can be used to show that the loop is stable for all additional phase (from u_K to u) within the following disk phase margin limits:

$$\mathrm{PM}_l = -2\cot(r), \quad \mathrm{PM}_u = 2\cot(r) \tag{11}$$

These are called disk margins due to a connection in the Nyquist domain. Specifically, stability of the interconnection in Figure 4 for all $\|\Delta\|_\infty < r$ implies that the open loop Nyquist curve of GK remains outside the disk containing –1 and with diameter passing through $[-GM_u, -GM_l]$. Figure 5 shows the disk margins for an example transfer function. The critical point (–1,0) is marked in red. The interval on the real axis between the disk (orange) and the critical point corresponds to the gain margin and the intersection of the disk and the circle around the origin with radius 1 marks the arc of the phase margin. For further information on disk margins the reader is referred to [5], for example.

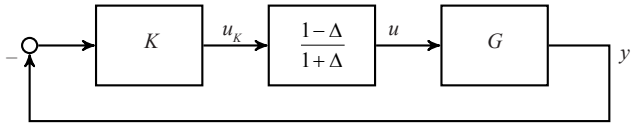

Figure 4 – Equivalent Input Disk Margin Interconnection

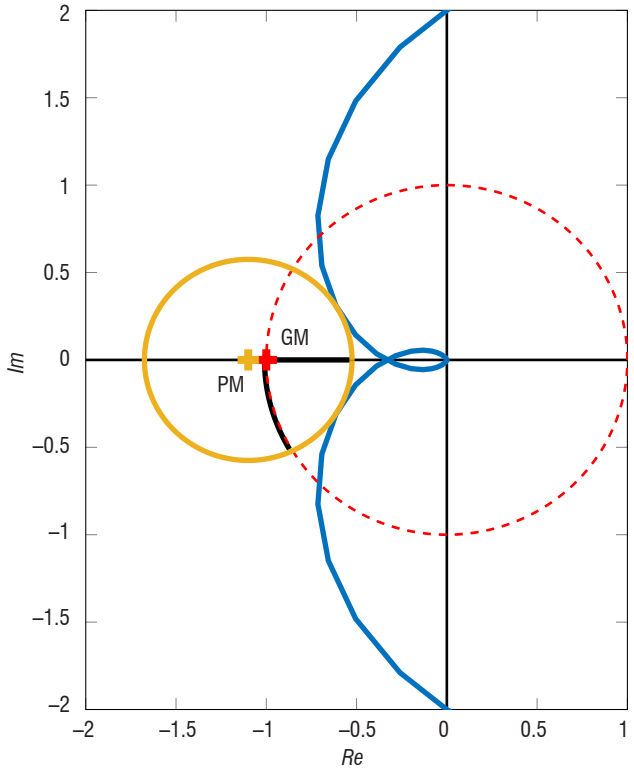

Figure 5 – Disk Margin in the Nyquist Plane

LPV Robustness Margins

Classical gain and phase margins are widely used as a standard formulation for robustness requirements in the aerospace industry. They do not require specific, detailed uncertainty models and, hence, these margins are easy to evaluate. Additionally, engineers have significant experience on the interpretation of the analysis results. At the same time, gain scheduling is a commonly used design method in aerospace. Since the classical margins are evaluated in the frequency domain, they cannot be directly applied to LPV systems due to the time varying nature of the dynamics. It is typical to simply evaluate the margins at "frozen" flight conditions. However, this fails to capture the effects of varying flight conditions. This motivates the proposed generalized robustness margins for LPV systems. The approach presented in this section provides two main extensions to the classical margins. A time domain worst-case metric can be used to formulate a generalized robustness margin for LPV systems. Additionally, this approach also considers the performance degradation before instability occurs.

LPV Disk Margins

The generalized disk margin interconnection in Figure 6 will be used for the analysis. This contains two significant differences from the previous disk margin interconnection in Figure 3. First, the plant G_ρ and controller K_ρ are allowed to be LPV systems. Here ρ is a parameter vector defining the flight condition. Second, an input d and output e are added in order to consider performance criteria. This corresponds to a plant input disturbance and plant output error. More generally, performance inputs/outputs can be included at any point in the feedback diagram depending on the specific application.

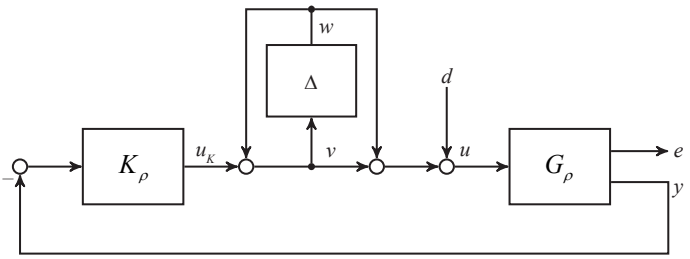

Figure 6 – Input Disk Margin Interconnection for LPV Systems

It is common to evaluate the classical margins with G_ρ and K_ρ evaluated at specific grid points of ρ. With a constant ρ, both the plant and controller are then LTI systems at the fixed operating condition. The disk margin analysis presented in Section "Disk Margins for LTI Systems" can be directly applied to this LTI interconnection. However, the resulting analysis does not consider the actual time varying nature of ρ. The approach proposed in this paper directly deals with the time varying operating conditions using the framework developed in [12].

Two basic robustness analysis problems will be considered, based on the LPV interconnection in Figure 6:

- **LPV Disk Margins**: Let Δ be an LTI uncertainty. Compute a stability margin r such that the LPV interconnection is stable for all $\|\Delta\|_\infty < r$ and all $\rho \in \mathcal{A}$.
- **Worst-Case Gain**: Again let Δ be an LTI uncertainty. In addition, assume that the uncertainty satisfies a given norm-bound $b < r$, *i.e.*, $\|\Delta\|_\infty < b$. Compute the worst-case gain from d to e over this set of uncertainties and all $\rho \in \mathcal{A}$.

The analysis requires a time-domain characterization of the uncertainty. Let $w = \Delta(v)$, where both w and v are assumed to be scalar signals, in order to simplify this discussion. The norm-bound $\|\Delta\|_\infty < b$ implies the following frequency-domain constraint on the input-output signals:

$$\begin{aligned} &\int_{-\infty}^{\infty} b^2 |V(j\omega)|^2 - |W(j\omega)|^2 d\omega = \\ &\int_{-\infty}^{\infty} V(j\omega)^* \left(b^2 - \Delta(j\omega)^* \Delta(j\omega)\right) V(j\omega) d\omega \geq 0 \end{aligned} \tag{12}$$

where $V(j\omega)$ and $W(j\omega)$ are the transforms of the signals $v(t)$ and $w(t)$. By Parseval's theorem [21], this inequality is equivalent to an infinite-horizon, time-domain constraint:

$$\int_0^{\infty} \begin{bmatrix} v(t) \\ w(t) \end{bmatrix}^T \begin{bmatrix} b^2 & 0 \\ 0 & -1 \end{bmatrix} \begin{bmatrix} v(t) \\ w(t) \end{bmatrix} dt \geq 0 \tag{13}$$

The causality of Δ implies that this constraint also holds for all finite intervals $[0,T]$, for all $v \in \mathcal{L}_2$, $w = \Delta(v)$ and $T > 0$ [12]. The time-invariance of Δ can be used to formulate a tighter constraint, as is standard in structured singular value (μ) analysis [9, 13]. Specifically, Δ is LTI and, hence, it commutes with any stable, minimum-phase LTI system D, *i.e.*, $D(s)\Delta(s) = \Delta(s)D(s)$. This property is the basis for the use of frequency-domain "D"-scale conditions in μ analysis [9, 13]. The equivalent time-domain formulation is obtained by noting that if $w = \Delta v$ then $Dw = \Delta Dv$. Hence, the filtered signals $(\tilde{v}, \tilde{w}) := (Dv, Dw)$ satisfy the same norm bound constraints as D. To simplify notation, combine the scalings D and stack the filtered signals as follows:

$$z := \begin{bmatrix} \tilde{v} \\ \tilde{w} \end{bmatrix} = \Psi \begin{bmatrix} v \\ w \end{bmatrix} \quad where \ \Psi := \begin{bmatrix} D & 0 \\ 0 & D \end{bmatrix} \tag{14}$$

As noted above, the filtered signals $(\tilde{v}, \tilde{w}) := (Dv, Dw)$ satisfy the same norm bound constraints as (v, w). This leads to the following time-domain inequality.

Definition 3.1
Let Δ be an LTI system satisfying $\|Delta\|_\infty < b$. In addition, let D be a stable, minimum phase LTI system. Define Ψ as in Equation 14 and $M = \begin{bmatrix} b^2 & 0 \\ 0 & -1 \end{bmatrix}$. Then Δ satisfies

$$\int_0^T z(t)^T M z(t) dt \geq 0 \tag{15}$$

for all $v \in \mathcal{L}_2$, $w = \Delta(v)$ and $T \geq 0$.

Equation 15 is a specific example of a time-domain *Integral Quadratic Constraint* (IQC). It is worth noting that IQCs provide a general framework, introduced in [7], for studying various uncertainties, such as infinite dimensional systems or hard non-linearities. There is an existing library of IQCs (Ψ, M) for particular classes of uncertainties. The (Ψ, M) given in Definition 3.1 is for the particular class of LTI norm-bounded uncertainty. The more general IQC framework can be used to obtain worst-case stability margins for other cases, e.g., systems with saturation. However, this paper will focus on norm bounded LTI uncertainties, in order to assess LPV disk margins.

LPV Worst-Case Gain

The (nominal) stability conditions of Section "Linear Parameter Varying Systems" can now be combined with the time domain constraint on the input/output behavior of the uncertainty block Δ. This can be used to assess the robust performance of an uncertain LPV system. First note that the LPV disk margin interconnection (Figure 6) is a special instance of the more general uncertain LPV system interconnection in Figure 7. Here, the nominal (not uncertain) LPV system T_ρ is connected to the uncertainty block. In addition, the dynamic filter Ψ, used to describe the IQC in Definition 3.1, is also appended to the diagram. The combined dynamics of T_ρ and Ψ are described by the following LPV system:

$$\begin{aligned} \dot{x} &= A(\rho)x + B_1(\rho)w + B_2(\rho)d \\ z &= C_1(\rho)x + D_{11}(\rho)w + D_{12}(\rho)d \\ e &= C_2(\rho)x + D_{21}(\rho)w + D_{22}(\rho)d \end{aligned} \tag{16}$$

The state vector combines the state of G and the state of Ψ, *i.e.*, $x = [x_G^T, x_\Psi^T]^T$. The perturbation block Δ is unknown and is not

considered for the purposes of analysis. Instead, w is treated as an external signal subject to the constraint on z given in Equation 15. This effectively replaces the precise relation $w=\Delta(v)$ by the imprecise time domain inequality.

The robust performance of this general uncertain LPV system (Figure 7) can be measured by the worst-case induced $\mathcal{L}_2$ gain from input d to output e over all uncertainties Δ satisfying the finite-time horizon constraint in (15). The following Theorem (from [12]) provides a matrix inequality condition to compute the upper bound on the worst case $\mathcal{L}_2$ -gain of $\mathcal{F}_u\left(T_\rho,\Delta\right)$.

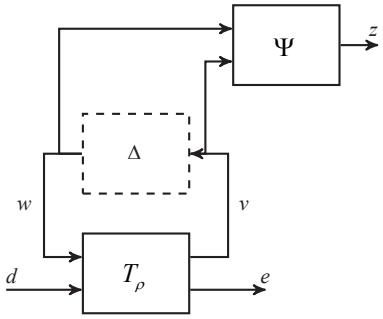

Figure 7 – Worst-Case Gain Analysis Interconnection

Theorem 3.2 (Extended Bounded Real Lemma [11])
Let $\mathcal{F}_u\left(T_\rho,\Delta\right)$ be well posed for any $\Delta\in IQC\left(\Psi,M\right)$. Then, the worst case gain of $F_u\left(T_\rho,\Delta\right)$ is upper bounded by $\gamma<\infty$ if there exists a continuously differentiable $P:\mathcal{P}\to\mathbb{S}^{n_x}$ and a scalar $\lambda>0$ such that the following conditions hold for all $\left(\rho,\dot\rho\right)\in\mathcal{P}\times\dot{\mathcal{P}}$:

$$P(\rho)>0, \tag{17}$$

$$\begin{bmatrix} P(\rho)A(\rho)+A(\rho)^TP(\rho)+\partial P(\rho,\dot\rho) & P(\rho)B_1(\rho) & P(\rho)B_2(\rho)\\ B_1(\rho)^TP(\rho) & 0 & 0\\ B_2(\rho)^TP(\rho) & 0 & -I\end{bmatrix}$$
$$+\lambda\begin{bmatrix}C_1(\rho)^T\\ D_{11}^T(\rho)^T\\ D_{12}^T(\rho)^T\end{bmatrix}M\begin{bmatrix}C_1(\rho) & D_{11}(\rho) & D_{12}(\rho)\end{bmatrix} \tag{18}$$
$$+\frac{1}{\gamma^2}\begin{bmatrix}C_2(\rho)^T\\ D_{21}(\rho)^T\\ D_{22}(\rho)^T\end{bmatrix}\begin{bmatrix}C_2(\rho) & D_{21}(\rho) & D_{22}(\rho)\end{bmatrix}<0$$

Proof. The proof is similar to Theorem 2.1. The uncertainty Δ is assumed to satisfy the IQC defined by $\left(\Psi,M\right)$, and therefore the signal z satisfies (15) for any $T>0$. Define a storage function $V\left(x,\rho\right)=x^TP(\rho)x$ as in the proof of Theorem 2.1. Left/right multiplication of Equation 18 by $\left[x^T,w^T,d^T\right]$ and $\left[x^T,w^T,d^T\right]^T$ leads to the following dissipation inequality

$$\dot V-d^Td+\lambda z^TMz+\frac{1}{\gamma^2}e^Te<0 \tag{19}$$

Integrating (19) over the finite time horizon $\left[0,T\right]$ and using the initial condition $x(0)=0$ along with the conditions $\lambda>0$ and $P(\rho)>0$ leads to the gain bound $\|e\|\le\gamma\|d\|$. This holds for any input $d\in\mathcal{L}_2$, admissible parameter trajectory $\rho\in\mathcal{A}$ and uncertainty $\Delta\in IQC\left(\Psi,M\right)$. Therefore the worst-case gain is upper bounded by γ.

The robustness analysis therefore consists in searching for decision variables, namely the matrix function $P(\rho)$, gain bound γ, and the constant λ, that lead to the feasibility of the conditions in Theorem 3.2. If the linear matrix inequality (LMI) conditions are feasible, then the system is stable for the selected uncertainty bound b. A bisection can be used to find the largest value of b for which the LMI is feasible. This largest uncertainty bound corresponds to the stability (disk) margin, denoted by r, for the LPV system. For example, the interconnection in Figure 6 is stable for all real gains from u_K to u in the interval $\left[\frac{1-r}{1+r},\frac{1+r}{1-r}\right]$. The other disk margin interpretations given in Section "Disk Margins for LTI Systems" have similar extensions to the LPV interconnection. The key point is that the plant and controller are LPV and the time-domain analysis enables the robustness with respect to LTI (disk-margin) uncertainty to be evaluated.

Theorem 3.2 can also be used to evaluate performance, in addition to the stability margin. In particular, it is important to emphasize that the performance can become unacceptable before the system becomes unstable. Thus, it is useful to evaluate the performance degradation for uncertainty bounds within the stability margin. In other words, a plot of worst-case gain vs. uncertainty bound b will approach infinity as $b\to r$. The performance degradation as the bound b increases provides additional useful information beyond simply knowing the stability margin r. It should also be mentioned that this approach can be used to obtain generalized delay margins for LPV systems, using existing time-domain IQCs for time delays. The work in [10] provides detailed information on IQCs for time-delayed LPV systems.

Numerical Implementation

The conditions in Theorem 3.2 involve infinite dimensional LMIs, *i.e.,* the conditions must hold for all $\rho\in\mathcal{P}$. In the case of System (1),depending only rationally on ρ, a guaranteed solution of the parameter dependent LMI conditions can be found, as proposed in [14]. In many practical applications, for example, the aeroelastic vehicle considered here, (1) depends arbitrarily on ρ. For this class of systems, an approximation of the parameter dependent constraints based on gridding is proposed in [19]. Specifically, the parameter space is approximated by a finite grid over $\left(\mathcal{P}\times\dot{\mathcal{P}}\right)$. It should be emphasized that the gridding approach is only an approximation for the parameter-dependent LMI conditions. Hence, no rigorous performance guarantees are provided by this approach, and special care must be taken when drawing conclusions. A pragmatic implementation of this approach is as follows: Enforce the LMI conditions on a "coarse" grid consisting of a small number of points, in order to reduce computation time. The resulting solution can then be checked on a "dense" grid of many points to ensure the accuracy of the solution. The SDP can be re-solved on a less coarse grid if required.

Another issue is that the matrix function P in Theorem 3.2 is itself parameter dependent. This function P can be expanded in terms of a finite number of basis functions:

$$P(\rho)=\sum_j^{n_\rho}b_j(\rho)P_j \tag{20}$$

where $b_j : \mathbb{R}^{n_\rho} \to \mathbb{R}$ can be any user-defined differentiable basis functions. The matrices P_j appearing in this expansion describe the function P with a (finite) number of decision variables. In general, there is no specific rule on how to choose the basis function. It has been reported that a similar parameter dependence as that in the system equations leads to satisfying results [2]. However, there is no scientific validation of this method in the literature. The choice of basis function used in the following application example will be described in Section "Robustness Analysis".

The final issue is the description of the IQC, which involves the scaling D. In μ-analysis the search over the D-scales is performed in the frequency domain on a grid of frequencies. This approach cannot be replicated for LPV analysis, since the condition in Theorem 3.2 is formulated in the time domain. Instead, many different D-scales, e.g., $\{D_i\}_{i=1}^{N}$ can be selected. Each D_i defines a valid IQC with corresponding filter Ψ_i. An approach for selecting basis functions for IQCs is proposed in [17]. The LMI conditions in Theorem 3.2 can be augmented in order to handle these multiple dynamic filters Ψ_i. The extended system then includes the additional dynamics of all Ψ_i. The corresponding LMI condition in (18) is modified to include one term corresponding to each selected D_i:

$$\sum_{i=1}^{N} \lambda_i \begin{bmatrix} C_{1i}(\rho)^T \\ D_{11i}(\rho)^T \\ D_{12i}(\rho)^T \end{bmatrix} M_i \begin{bmatrix} C_{1i}(\rho) & D_{11i}(\rho) & D_{12i}(\rho) \end{bmatrix} \qquad (21)$$

The constants λ_i are decision variables each of which must be ≥ 0. The output state matrices $(C_{1i}(\rho), D_{11i}(\rho), D_{12i})$ corresponding to the output z_i of filter Ψ_i. The analysis includes a search for the constants λ_i that lead to the feasibility of the LMI conditions in Theorem 3.2. It is worth noting that, in principle, Ψ and M do not have to be LTI but could potentially be LPV. However, the use of LPV (Ψ, M) has not been fully developed in the literature and will not be pursued here.

Application on a Flexible Aircraft

The proposed method is used to evaluate the LPV robustness margins of a flutter suppression controller for a flexible aircraft. The airframe is a small, radio-controlled aircraft denoted *mini-MUTT*, as shown in Figure 8. The design is based on Lockheed Martin's Body Freedom Flutter vehicle [4]. The mini-Mutt has a mass of 6.7 kg and a wing span of 3 meters. It was built completely in-house at the University of Minnesota to study the usage of active control for suppressing detrimental structural and aerodynamic interactions. These undesired interactions lead to a phenomenon called flutter, which is an unstable oscillation that can potentially destroy the aircraft. Given the catastrophic consequences of flutter, it is paramount to have an insightful and accurate robustness metric available.

Figure 8 – mini MUTT

System Description

The modeling of the aircraft incorporates structural and rigid body dynamics, as well as aerodynamics. The procedure can be found in [15]. The final model which is used is adapted from [11] and describes the longitudinal dynamics for straight and level flight. The system has a total of six states as well as one input and three output signals.

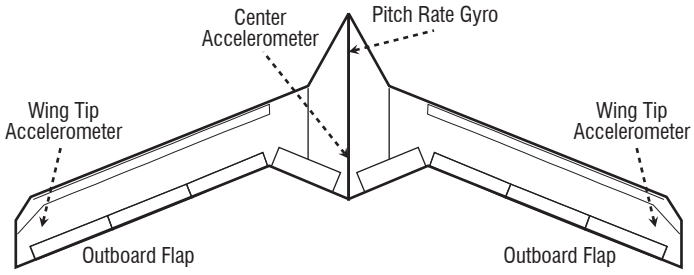

Figure 9 – Schematic Overview

A schematic overview of the aircraft is depicted in Figure 9, showing the available sensors and actuators. The aircraft has a total of 8 flaps on the back of the wing. The body flaps are unused in this example, while the inner two are the aileron and elevator, respectively. The flutter suppression controller has full authority over the outboard flap deflection denoted by δ, such that $u = \delta$. The plant output signals are the pitch rate q and the vertical acceleration at the center of gravity a_{CG} and the wing tips a_{WT}, such that $y = [q\, a_{CG}\, a_{WT}]$. A short period approximation of the full model as proposed in [16] is used. The first two states of the state space representation are associated with the rigid body dynamics and consist of the angle of attack α and pitch rate q. The remaining states represent the generalized displacement and velocity of the first flexible mode, denoted by η and $\dot{\eta}$, respectively. Therefore, the approximated plant model is of 4th-order and consists of the four states $\alpha, q, \eta, \dot{\eta}$. The dynamics strongly depend on the airspeed and it is therefore straightforward to represent the aircraft model as a parameter varying model. Specifically, the airspeed is assumed to be a measurable exogenous signal, which can be used as the scheduling parameter $\rho(t)$. Additionally, the sensor and actuator dynamics and the assumed time delay as described in [16] are included, leading to the final 6th-order LPV model.

The LPV controller is mainly based on the H_∞ design, which is also proposed in [16]. In this work, the airspeed is assumed to be constant, 30 m/s. To adapt the controller design to the LPV description of the system, the loopshaping approach can be systematically extended using the synthesis algorithm provided in [20]. Weighting filters can be used to shape the individual transfer functions of the individual performance channels. The modal velocity $\dot{\eta}$ of the first flexible mode is used as a non-measurable performance output. Since the main objective of the flutter suppression controller is to attenuate the mode, this can be achieved by pushing down the peak in the associated transfer function using a constant weighting filter.

Robustness Analysis

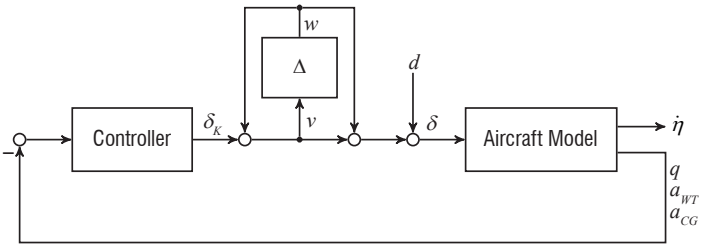

Figure 10 – Equivalent Input Disk Margin Interconnection

The LPV robustness margin analysis is performed on the closed-loop system of the aircraft and the LPV flutter suppression controller as shown in Figure 10. The parameter range is assumed to be $\rho = [20,\ldots,40]$ m/s and the parameter variation rate is bounded by ± 10 m/s^2. The worst-case performance is computed for increasing values of b by solving the LMI conditions in Theorem 3.2. The results are then normalized by the $\mathcal{L}_2$ gain of the nominal system $(b = 0)$. Let us recall that a norm bounded uncertainty is assumed to satisfy an IQC of the form

$$\Psi_1 = I_2 \qquad M = \begin{bmatrix} b^2 & 0 \\ 0 & -1 \end{bmatrix} \tag{22}$$

A second filter with simple first order dynamics

$$\Psi_2 = \begin{bmatrix} \frac{1}{s+1} & 0 \\ 0 & \frac{1}{s+1} \end{bmatrix} \tag{23}$$

is added to the analysis. Let us recall that, in general, it is possible to choose any stable minimum phase LTI system as a basis for the filter Ψ. However, including more complicated filters into the analysis did not lead to a significant improvement of the results. Initially, a constant matrix function P is used for the LMI conditions in Theorem 3.2. The analysis is then repeated, using linear and quadratic basis functions for the approximation of $P(\rho)$, *i.e.*, $P(\rho) = P_0 + \rho P_1$ and $P(\rho) = P_0 + \rho P_1 + \rho^2 P_2$. As a comparison, for each value of b the largest worst-case gain of the LTI systems over all individual grid points is computed, using the μ-Analysis framework and the Matlab function `wcgain`. Specifically, for a fixed value of b the LTI worst-case gain is computed at each grid point. The largest gain of all grid points is then plotted as a function of the uncertainty norm bound b.

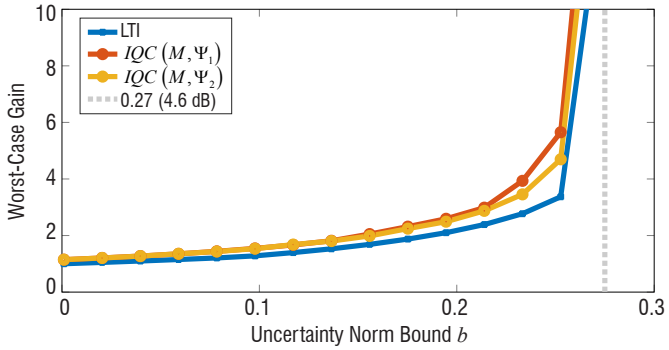

Figure 11 – Norm Bounded Uncertainty Worst-Case Gain

Evaluation

The optimization algorithm could not find any feasible solutions using a constant P and a linear basis functions. The analysis results using quadratic basis functions are shown in Figure 11. It can be seen that the worst-case gain using `wcgain` as well as the proposed method for LPV systems converges to the gain of the nominal plant $(b = 0)$. The gain slowly increases for uncertainty bounds below 0.1. Even further, the upper bound on the worst-case LPV gain is very close to the lower bound given by the largest LTI worst-case gain over all grid points. Using a constant matrix P as well as affine parameter dependence clearly introduces too much conservatism. Additional basis functions for the matrix function $P(\rho)$, such as a third-order polynomial were tested as well, but did not lead to a significant improvement of the results. Adding an additional IQC with internal dynamics shows only minimal improvement of the results. Both curves indicate an upper bound for the robustness margin of $b_{max} \approx 0.27$, corresponding to a real gain at the plant input of about 1.7 (4.6 dB). In comparison, the lowest LTI input-disk margin over all individual grid points is 4.9 dB. Let us recall that evaluating the classical LTI margins at each grid point has only been assumed to give a valid statement for the overall LPV system, so far. However, the results obtained by the worst-case LPV gain are very close to the LTI margin results, which indicates that the LTI analysis is indeed a useful first indicator of the LPV robustness in this application.

Conclusion

The IQCs framework can be used to extend classical robustness margins to LPV systems. The approach is independent from the plant and therefore no specific uncertainty modeling is required. Simultaneous gain and phase variations can be expressed using a norm bounded LTI perturbation block in connection to the nominal LPV system. The worst-case gain metric can be used to determine the robustness margins in the time domain, as well as the robust performance. The applicability was demonstrated on a flutter suppression controller ■

Acknowledgments

The work was supported by the National Science Foundation under Grant No. NSF-CMMI-1254129 entitled "CAREER: Probabilistic Tools for High-Reliability Monitoring and Control of Wind Farms".

Acronyms

IQC (Integral Quadratic Constraint)
LMI (Linear Matrix Inequality)
LPV (Linear Parameter Varying)
LTI (Linear Time Invariant)
SDP (Semidefinite Program)
SISO (Single Input/Single Output)

References

[1] P. APKARIAN, P. GAHINET - *A Convex Characterization of Gain-Scheduled H/Sub ∞ / Controllers.* IEEE Transactions on Automatic Control, 40(5):853-864, 1995.

[2] G. J. BALAS - *Linear, Parameter-Varying Control and its Application to a Turbofan Engine.* International Journal of Robust and Nonlinear Control, 12(9):763-796, 2002.

[3] D. BATES, I. POSTLETHWAITE - *Robust Multivariable Control of Aerospace Systems.* IOS Press, 8th edition, 2002.

[4] J. BERANEK, L. NICOLAI, M. BUONANNO, E. BURNETT, C. ATKINSON, B. HOLM-HANSEN, P. FLICK - *Conceptual Design of a Multi-Utility Aeroelastic Demonstrator*. 13th AIAA/ISSMO Multidisciplinary Analysis Optimization Conference, 3:2194-2208, 2010.

[5] J. D. BLIGHT, R. L. DAILEY, D. GANGSAAS - *Practical Control Law Design for Aircraft Using Multivariable Techniques.* International Journal of Control, 59(1):93-137, 1994.

[6] C. A. DESOER, M. VIDYASAGAR - *Feedback Systems: Input-Output Properties.* Academic Press, New York, 1975.

[7] A. MEGRETSKI, A. RANTZER - *System Analysis via Integral Quadratic Constraints.* IEEE Transactions on Automatic Control, 42(6):819-830, 1997.

[8] A. PACKARD - *Gain Scheduling via Linear Fractional Transformations.* Systems & Control Letters, 22(2):79-92, 1994.

[9] A. PACKARD, J. DOYLE - *The Complex Structured Singular Value.* Automatica, 29(1):71-109, 1993.

[10] H. PFIFER, P. SEILER - *Integral Quadratic Constraints for Delayed Nonlinear and Parameter-Varying Systems.* Automatica, 56:36-43, 2015.

[11] H. PFIFER, P. SEILER - *Less Conservative Robustness Analysis of Linear Parameter Varying Systems Using Integral Quadratic Constraints.* International Journal of Robust and Nonlinear Control, 26(16):3580-3594, 2016.

[12] H. PFIFER, P. SEILER - *Robustness Analysis of Linear Parameter Varying Systems Using Integral Quadratic Constraints.* International Journal of Robust and Nonlinear Control, 25(15):2843-2864, 2015.

[13] M. G. SAFONOV - *Stability and Robustness of Multivariable Feedback Systems.* MIT Press, Cambridge, MA, USA, 1980.

[14] C. W. SCHERER - *LMI Relaxations in Robust Control.* European Journal of Control, 12(1):3-29, 2006.

[15] D. K. SCHMIDT, W. ZHAO, R. K. KAPANIA - *Flight-Dynamics and Flutter Modeling and Analyses of a Flexible Flying-Wing Drone*. Proceedings of the AIAA SciTech Conference, :4-8, 2016.

[16] J. THEIS, H. PFIFER, P. J. SEILER - *Robust Control Design for Active Flutter Suppression.* AIAA Atmospheric Flight Mechanics Conference, p.1751, 2016.

[17] J. VEENMAN, C. W. SCHERER, H. KÖROGLU - *Robust Stability and Performance Analysis Based on Integral Quadratic Constraints.* European Journal of Control, 31:1-32, 2016.

[18] J. VEENMAN, C. W. SCHERER, I. E. KÖSE - *Robust Estimation with Partial Gain-Scheduling Through Convex Optimization.* Control of Linear Parameter Varying Systems with Applications, pages 253-278. Springer US, Boston, MA, 2012.

[19] F. WU - *Control of Linear Parameter Varying Systems.* Dissertation, University of California at Berkeley, 1995.

[20] F. WU, X. H. YANG, A. PACKARD, G. BECKER - *Induced L_2-Norm Control for LPV System with Bounded Parameter Variation Rates.* American Control Conference, Proceedings of 1995, 1995.

[21] K. ZHOU, J. C. DOYLE, K. GLOVER - *Robust and Optimal Control.* Prentice Hall, New Jersey, 1996.

Ann-Kathrin Schug graduated from the Hamburg University of Technology (TUHH), Germany in 2016. In early 2016 she joined the Aerospace Engineering and Mechanics Department of the University of Minnesota to work on robust control of a flexible aircraft. She is now a Ph.D. student at the Institute of Control Systems (TUHH) working on distributed control of spatially-interconnected systems.

Peter Seiler received his Ph.D. from the University of California, Berkeley in 2001. His graduate research focused on coordinated control of unmanned aerial vehicles and control over wireless networks. From 2004-2008, he worked at the Honeywell Research Labs on various aerospace and automotive applications including the redundancy management system for the Boeing 787, sensor fusion algorithms for automotive active safety systems and re-entry flight control laws for NASA's Orion vehicle. Since joining the University of Minnesota in 2008, he has been working on fault-detection methods for safety-critical systems and advanced control techniques for wind turbines and unmanned aircraft.

Harald Pfifer received his Ph.D. from the Technical University Munich, Germany in 2013. From 2008 till 2013, he has been a Research Associate with the Institute of Robotics and Mechatronics, German Aerospace Center (DLR), Oberpfaffenhofen, Germany. From 2013 to 2016 he has been a post-doctoral associate at the Aerospace Engineering and Mechanics Department of the University of Minnesota after which he joined the University of Nottingham as an assistant professor. His main research interests include aeroservoelastic control, modeling of uncertain dynamical system and robust and linear parameter varying control.